Reduction of SLL in a Square Horn Antenna in Presence of Metamaterial Surfaces by Using of Particle Swarm Optimization

Anis Moradi
MSc. Student
Dept. of Communications and Electronics,
Shiraz University
Shiraz, Iran
Email: moradi_a539@yahoo.com

Farzad Mohajeri
Assistant Professor
Dept. of Communications and Electronics,
Shiraz University
Shiraz, Iran
Email: mohajeri@shirazu.ac.ir

Abstract—**Metamaterial surfaces with a low refractive index have been recently proposed in the design of the low side lobe level horn antennas based on engineering dispersion method. This paper explores a linearly polarized square horn antenna in the Ku-band for communication satellite reflector antennas. We study the designs of broadband metasurfaces and their use as coating layers on the interior E-plane walls of the horn. The design process includes combining the Particle Swarm Optimization technique with a full wave electromagnetic solver to model dispersion-engineered metasurfaces with surface impedance characteristics that support the desired hybrid modes. The obtained optimized metasurface is a low refractive index metamaterial with negligible losses that improves the conventional horn properties over the frequency band. The symmetric far field radiation patterns, the low side low levels and cross polarization levels and the aperture field distributions verify the hybrid mode operation of the horn. Moreover, this technique promises for a lighter horn with an easier manufacturer method compared with the conventional dielectric core loaded and corrugated horns.**

Keywords-Metasurfaces; low refractive index; surface impedance; hybrid mode horns; horn antennas; Particle Swarm Optimization (PSO).

I. INTRODUCTION

Horn antennas are widely used as a feed element for large radio astronomy, satellite tracking, radar and high power microwave systems due to their high power handling properties [1].Up to now, many different forms of horns have been introduced to improve the radiation properties. One popular type of horn antennas is hybrid mode horn which can radiate low side lobe and low cross polarization level [2],[3].The first hybrid mode horn were introduced around 1966 including corrugated horn [4]-[6] and the dielguide feed[7] and have been extensively developed since then. In 1983 the dielectric core horn, including a dielectric core separated from the conducting walls by a small air gap was introduced [8].The strip-loaded horn, realized by loading the dielectric coating with a grating of strips, was proposed in 1985[9].Loading trifurcations inside the horn improves the side lobe level in the E-plane walls [10] but it still has large side lobes and back lobes and can't be used in dual polarization applications. The corrugated horns have a large mass specially at low frequencies and are expensive to manufacture. Although dielectric loaded horns offer a wide bandwidth, they aren't used extensively in satellite communications for reasons like dielectric losses, reflection from the dielectric-air aperture and their large mass.

Electromagnetic Metamaterials offer a new technique in designing hybrid mode horn antennas. Lier and Shaw presented a new type of hybrid mode horn designs. This type of horn is based on low refractive index metamaterial wall lining [11]. Horn antenna characteristics are improved by incorporating these liners into the design [12] and the material dispersion follows a Drude-type behaviour, which confirms this material can be realized over a large bandwidth [13]. Despite the good performance of this horn, it lacked the metamaterial which implemented the low refractive index properties. Recently, an efficient optimization technique has been proposed in [14]. This technique is used to design a broadband metasurface which satisfies the balanced hybrid mode condition. A metamaterial-based square horn antenna was designed to operate in the C-band in [15], [16]. A wire grid metamaterial was placed on the interior walls, lining the walls perpendicular to the E-plane walls and forcing the electric field to zero at the edges of the horn aperture. It yields a tapered electric field distribution at the E-plane walls and leads to low side lobe levels and symmetric radiation patterns. In paper [17] a metahorn with the metamaterial liners on all for interior walls including the E-planes and the H-planes is presented which shows low side lobe levels and low cross polarizations but it can be still improved in cost and weight as will be mentioned below.

In this paper we present the design, simulation and characterization of a metahorn which is loaded by metamaterial liners only on the E-plane walls. So besides it maintains the low side lobe levels and the symmetric radiation patterns of the lately presented metahorns, it can be implemented with lower manufacturing costs and a lighter weight. In section II, we describe the design of the metamaterial structure where an optimized broadband metasurface is proposed. Section III presents the metahorn and its basic structure. In section IV, the simulation results are given. Finally, in section V, conclusions are drawn.

II. METAMATERIAL SURFACE DESIGN

Recently, metasuraces have been realized by using different type of structures like frequency selective surface screens on top of a dielectric layer [18] and wire grid liners [19].

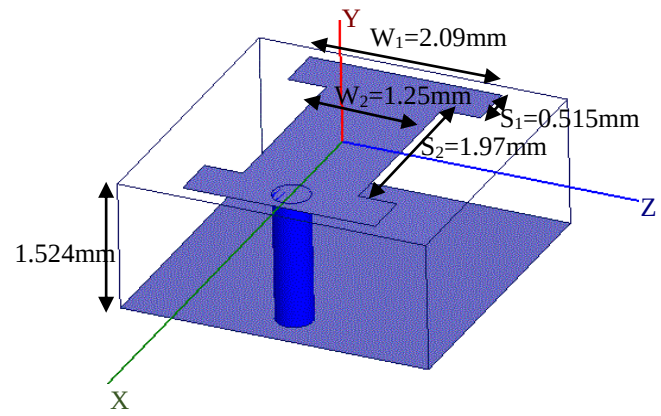

(a)

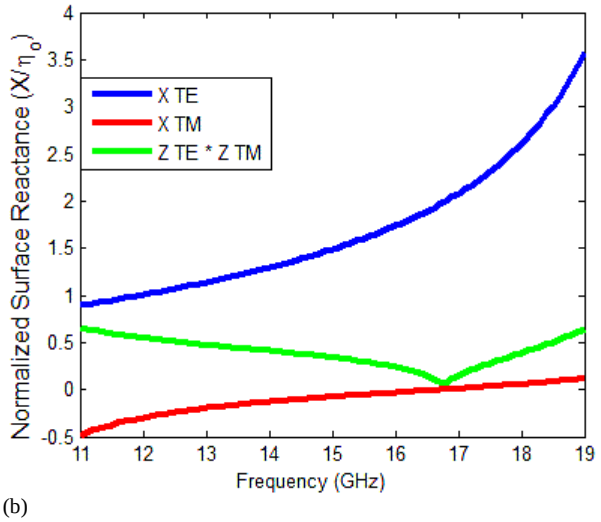

(b)

Figure 1. (a) Geometry of the optimized unit cell that supports a broadband balanced hybrid mode. (b) Normalized surface reactance for TE and TM polarizations.

Here we present the design of broadband metasurfaces incorporating engineering dispersion to provide the appropriate boundary condition inside the horn and achieve a new type of hybrid mode horn operating in the Ku band with low side lobe levels, low cross polarizations and symmetric radiation patterns. The printed circuit board technique is a proper way to construct the metasurfaces because it reduces the cost and weight of the antenna as well as providing the ideal wideband performance of the antenna.

The metasurface consists of periodic unit cells which are much smaller than the operating wavelength so we can describe the metasurface by its effective surface impedances.

The unit cell includes a metal patch on the top surface of the dielectric substrate and a via connects the patch to the ground plane at the bottom of the substrate. The location of vias is important because they interact with the incident waves under TM polarized mode and taper the electric field on the E-plane walls. They are located at the center line of the unit cell to provide the symmetric property of the unit cell.

Fig. 1(a) shows the geometry and dimensions of the optimized metasurface. The unit cell is square with the periodicity of 3.35 mm in both x and z directions. The thickness of the substrate is 1.524 mm. The dimensions of the patches are W_1 = 2.09 mm, W_2 = 1.25 mm, S_1 = 0.515 mm and S_2 = 1.97 mm. The FSS patch is chosen to be symmetric to reduce the cross polarizations. The substrate used for this prototype was Rogers 4003 with dielectric constant of 3.35 and loss tangent of 0.0027.

In this study we use efficient optimization technique to achieve the design goals because the conventional analytical-based approaches are not feasible due to the difficult multi-objective criteria that must be met. Various optimization tools can be employed to synthesize the matamaterial cell. In this work we combined full wave simulation techniques with the Particle Swarm Optimization (PSO) tool [20] to achieve the design goals over a wide frequency band. Furthermore, we considered the fabrication confinements in the optimization to obtain a practical device with a simple manufacture.

We should satisfy the condition $Z^{TM} * Z^{TE} = \eta_0^2$ to achieve the hybrid mode condition. We used a plane wave model and by extraction of the complex reflection coefficients Γ^{TM} and Γ^{TE} through simulation, we calculated the surface impedances Z^{TM} and Z^{TE} of the metasurface according to (1), (2), (3) and (4) [21].

$$Z^{TM} = R^{TM} + jX^{TM} = \frac{-E_z}{H_x} = \eta^{TM}\frac{1+\Gamma^{TM}}{1-\Gamma^{TM}} \quad (1)$$

$$Z^{TE} = R^{TE} + jX^{TE} = \frac{E_x}{H_z} = \eta^{TE}\frac{1+\Gamma^{TE}}{1-\Gamma^{TE}} \quad (2)$$

$$\eta^{TM} = \eta_0 \cos\theta_1 \quad (3)$$

$$\eta^{TE} = \frac{\eta_0}{\cos\theta_1} \quad (4)$$

R^{TM} and R^{TE} are the surface resistance while X^{TM} and X^{TE} are the surface reactance. θ_1 is the angle of the incident wave and we choose it 80°. In Fig. 1(b), we observe both X^{TE} and X^{TM} are relatively dispersive but it closely satisfies the hybrid mode condition within the frequency band which means we can achieve low side lobe levels and symmetric radiation patterns. We can compute the effective refractive index of the unit cell through (5) [21].

$$n_{eff} = \sin\theta_1 (1 - \frac{Z^{TM}}{Z^{TE}})^{-\frac{1}{2}} \quad (5)$$

As shown in Fig. 2, the real part of the effective refractive index is below unity all over the frequency bandwidth and follows a Drude-like dispersion which makes this metasurface practical to be used in the metahorn [22]. Moreover, the imaginary part of the refractive index is almost zero with the precision of (1e -4). It indicates that the intrinsic loss of the metamaterial is very small and inconsiderable.

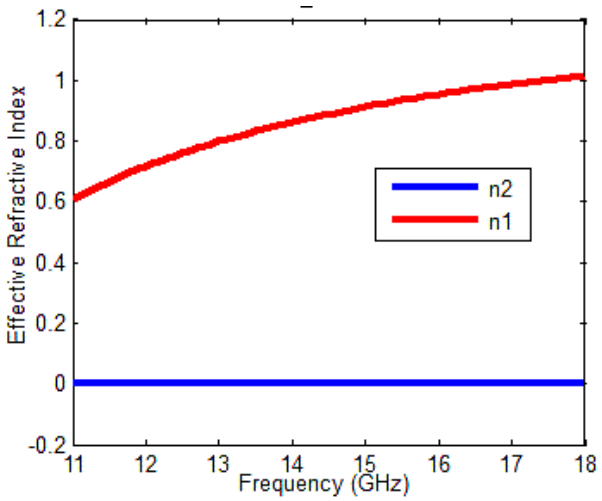

Figure 2. The effective refractive index of the unit cell (n1 - j n2). The real part of the index n1 is below unity across the entire band. The imaginary part n2 exhibit an inconsiderable loss, ranging from 1.5× 10^{-3} at 11 GHz to 6.6 × 10^{-4} at 18 GHz.

III. METAHORN STRUCTURE

The square horn considered has a 75 × 75 mm aperture. The total length is 121 mm. The feed waveguide is WR62 connected to a linearly tapered waveguide followed by a square waveguide with the dimensions 15.8 × 15.8 mm and length of 50 mm as shown in Fig.3. These dimensions lead to a peak gain around 20 dB. The metamaterial liners are placed on the interior E-plane walls extending all the way from the throat to the radiating aperture of the horn. The waveguide port is excited by the TE_{10} waveguide mode in the simulation.

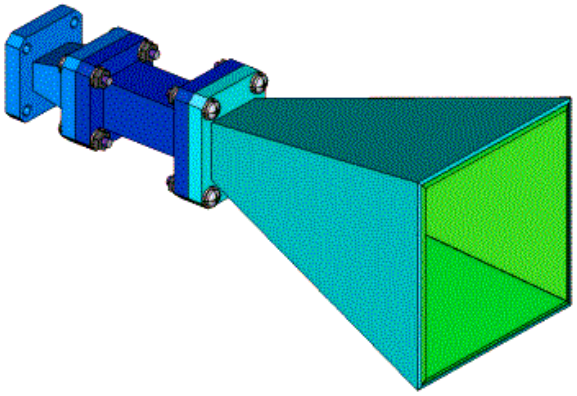

Figure 3. Horn geometry [17].

IV. THE SIMULATION RESULTS

Figs. 4 - 6 show radiation patterns of the metahorn at 12, 15, 18 GHz in the E-plane, H-plane, and φ= 45° plane cut, respectively. The radiation patterns in all the three planes are nearly similar and the side lobe levels are below -24 dB across the entire bandwidth. The liner reduces the side lobes in the E-plane wall by more than 15 dB, confirming that tapered electric field distributions at the edges of the aperture are achieved and the radiation patterns are symmetric. Such a metahorn with enhanced radiation efficiency can be used as a feed for reflectors.

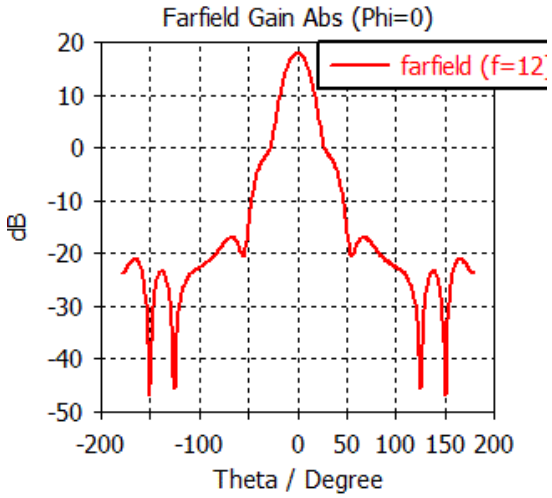

(a)

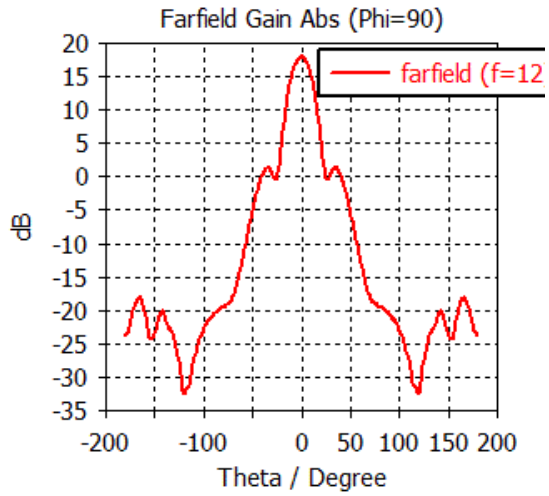

(b)

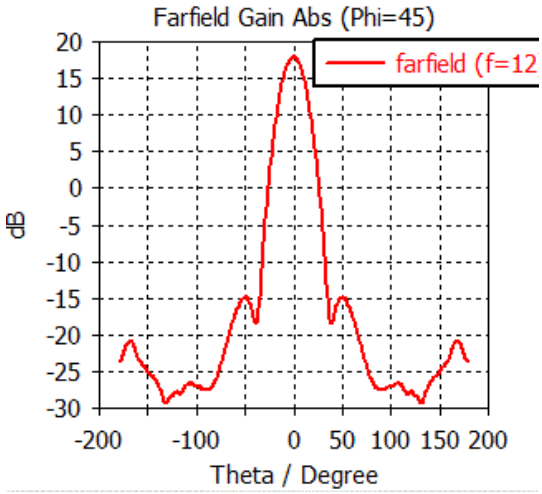

(c)

Figure 4. Simulated radiation patterns of a metahorn in (a) the E- plane, (b) H-plane and (c) φ= 45° plane. The operating frequency is 12 GHz.

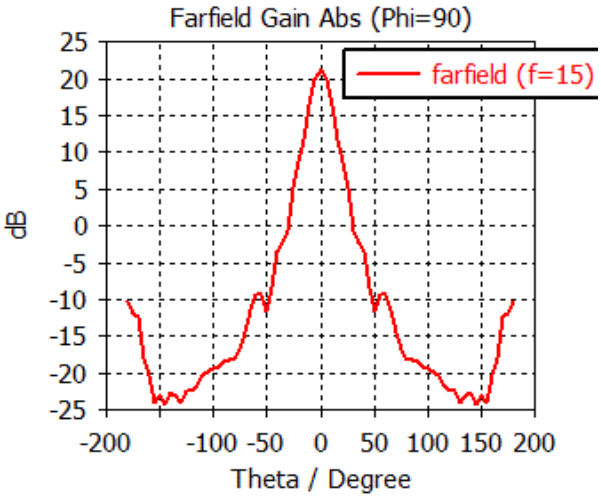

(b)

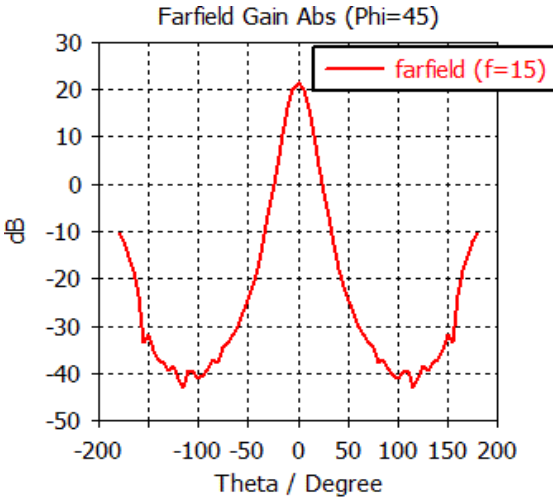

(c)

Figure 5. Simulated radiation patterns of a metahorn in the (a) E- plane, (b) H-plane and (c) φ= 45° plane. The operating frequency is 15 GHz.

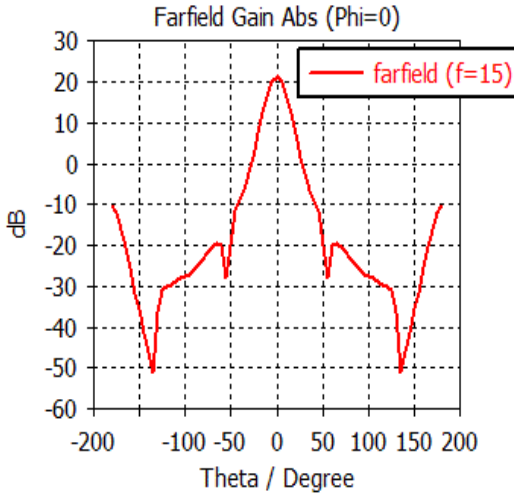

(a)

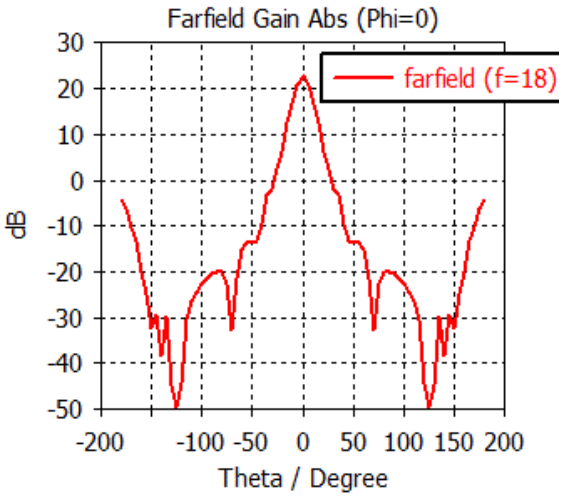

(a)

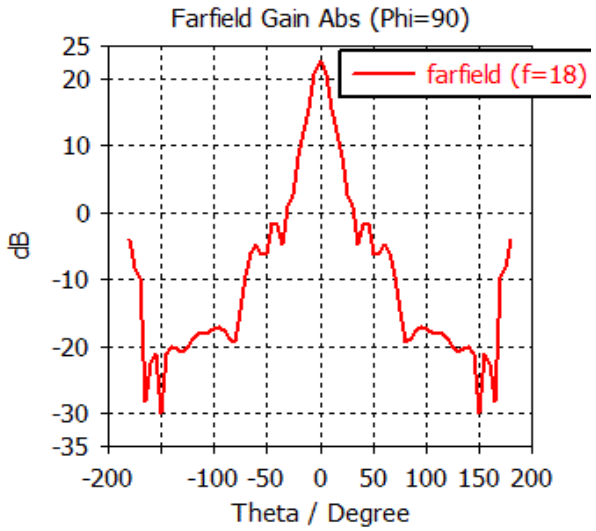

(b)

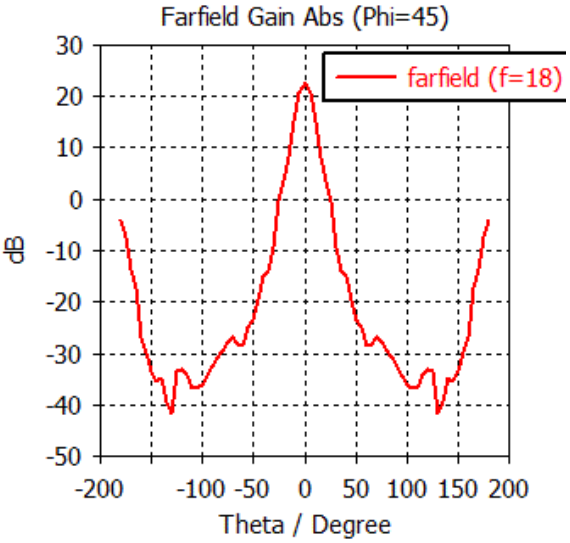

(c)

Figure 6. Simulated radiation patterns of a metahorn in the (a) E-plane, (b) H-plane and (c) φ= 45° plane. The operating frequency is 18 GHz.

Fig.7 shows the simulated reflection coefficients (s11) for the horn with and without the liner, respectively. It is clear that by placing the liner in the horn the amount of return loss is still acceptable while it simultaneously improves the radiation properties of the antenna.

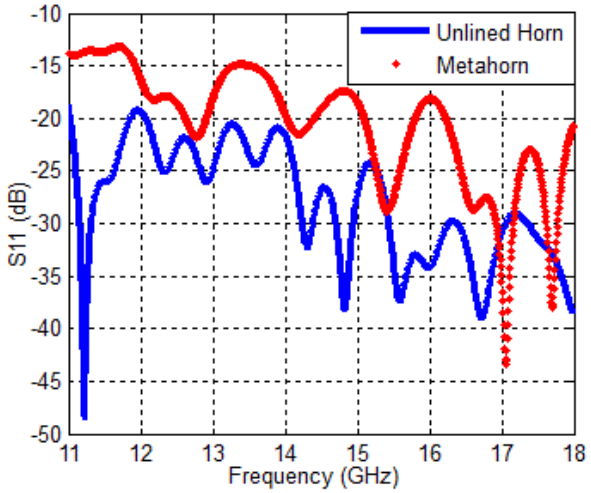

Figure 7. The reflection coefficients (s11) of the metahorn and the unlined horn.

Fig. 8(a) shows the 3-D radiation patterns of the metahorn at 12, 15, 18 GHz, respectively. The symmetry of the radiation patterns is obvious. On the contrary, the radiation patterns of an unlined square horn show considerable side lobes in the E-plane as shown in Fig. 8(b). These simulation results validate the presented metasurface design approach and confirm that the metamaterial liner improves the radiation characteristics of the horn.

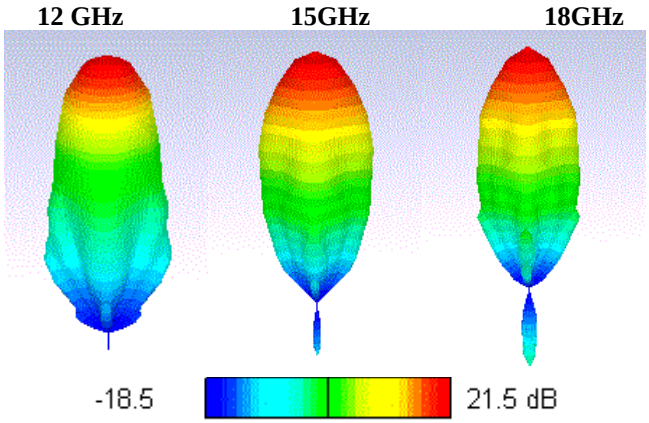

(a)

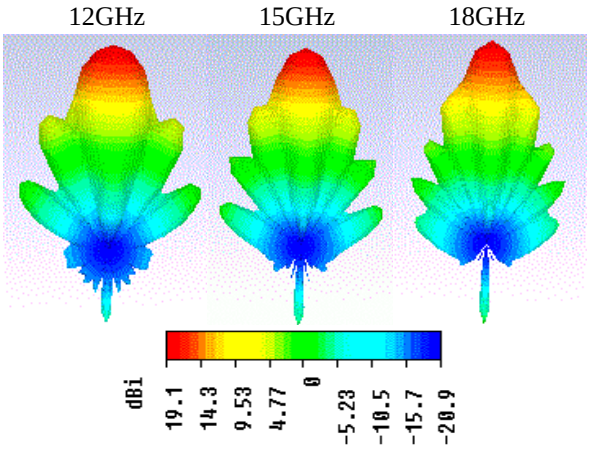

(b)

Figure. 8. (a) Simulated 3-D radiation patterns of the metahorn at 12, 15, 18 GHz, respectively. Symmetric patterns with low side lobe levels are obtained across the bandwidth. (b) Simulated 3-D radiation patterns of an unlined horn with the same dimensions at 12, 15, 18 GHz, respectively.

V. CONCLUSION

In this paper, we analyzed broadband hybrid metasurfaces using PSO optimization technique. We obtained the desired surface impedances by engineering the dispersion properties of the metasurfaces. By loading the metasurfaces as a liner in a square horn antenna, the field distribution across the aperture of the horn changed to a tapered field as shown in fig. 9. We observed balanced hybrid mode performance and the metahorn radiated symmetric radiation patterns with low side lobe levels all over the frequency bandwidth. Such broadband hybrid mode metahorns are appropriate for satellite communications.

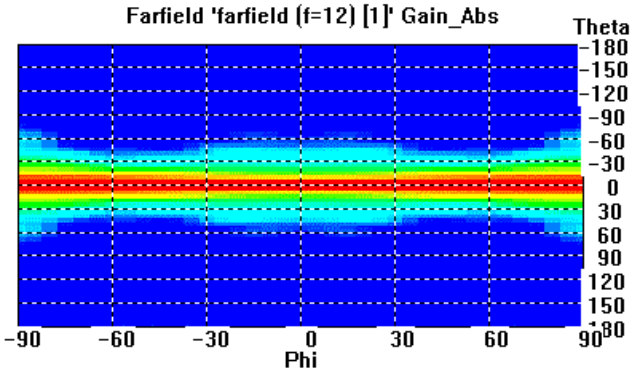

(a)

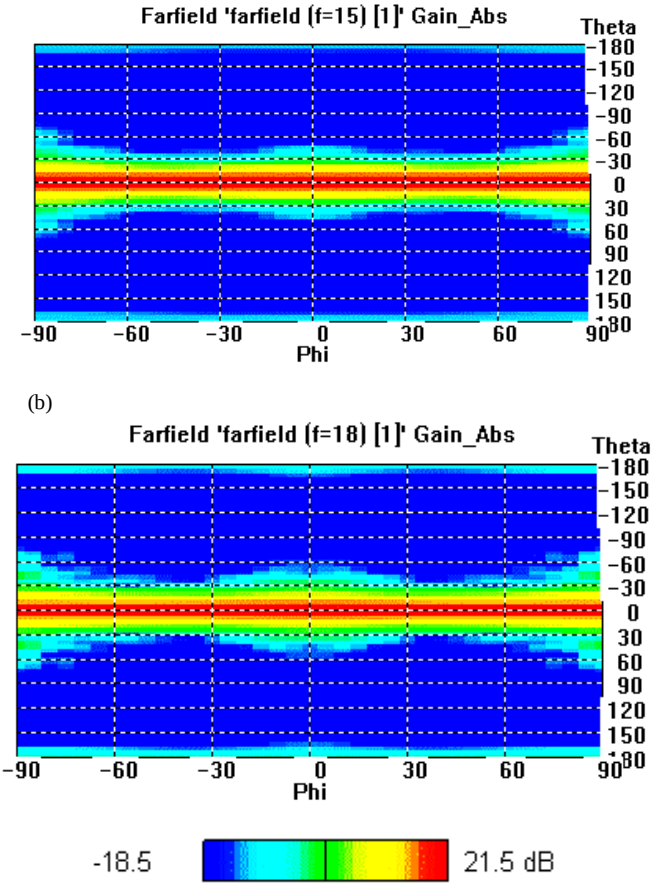

(b)

(c)

Figure. 9. Simulated electric field distributions at the aperture of the metahorn and an unlined horn. The operating frequencies are 12, 15, 18 GHz, in (a) , (b), and (c) respectively. The fields are tapered at each E-plane wall.

REFERENCES

[1] balanisJ. Clerk Maxwell, "A Treatise on Electricity and Magnetism", 3rd ed., vol. 2. Oxford: Clarendon, 1892, pp.68–73.

[2] E.LierandP.S.Kildal,"Soft and hard horn antennas, " IEEE Trans. Antennas Propag., vol. 36, no. 8, pp. 1152–1157, Aug. 1988.

[3] E. Lier, "Review of soft and hard horn antennas, including metamaterial-based hybrid-mode horns," IEEE Antennas Propag. Mag. , vol. 52, no. 2, pp. 31–39, Apr. 2010.

[4] A. J. Simmons and A. F. Kay, "The scalar feed-A high performance feed for large paraboloidal reflectors," in Inst. Elec. Eng. Conf. Publ. 21, June 1966, pp. 213-217.

[5] H. C. Minnett and B. MacA. Thomas, "A method of synthesizing radiation patterns with circular symmetry," ZEEE Trans. Antennas Propagat.. vol. AP-14, pp. 654-656, Sept. 1966.

[6] V. H. Rumsey, "Horn antennas with uniform power patterns around their axis," ZEEE Trans. Antennas Propagat., vol. AP-14, pp. 656-658, Sept. 1966.

[7] H. E. Bartlett and R. E. Mosely, "Dielguides-Highly efficient low noise antenna feeds," Microwave J., vol. 9, pp. 53-58, Dec. 1966.

[8] P. J. B. Clarricoats, A. D. Olver, and M. S. A. S. Rizk, "A dielectric loaded conical feed with low crosspolar radiation," in Proc. URSI Symp. EM Theory, Santiago de Compostela, Spain, Aug. 23-26, 1983, pp. 351-354.

[9] E. Lier, T. Schaug-Pettersen, and J. A. Aas, “New classes of hybrid mode antennas-Alternatives to corrugated horn feeds,” in Proc. ZEEEAJRSZSymp., Vancouver, BC, June 1985, sec. B-18-6, p. 241.

[10] Peace, G. M. & Swartz, E. E. Amplitude compensated horn antenna. Microwave J.7,66-68, 1964.

[11] Lier, E.: ‘Horn antenna, waveguide or apparatus including low index dielectric material’, (patent pending)

[12] Lier, E. & Shaw, R. K. Design and simulation of metamaterial-based hybrid-mode horn antennas.Electron. Lett.44,1444 1445 (2008

[13] Q. Wu, C. P. Scarborough, D. H. Werner,E. Lier, and X. Wang, “Design synthesis of metasurfaces for bro adband hybrid-mode horn antennaswith enhanced radiation pattern and polarization characteristics,” IEEE Trans. Antennas Propag., vol. 60, no. 8, pp. 3594–3604, Aug. 2012.

[14] Rotman, W. Plasma simulation by artificial dielectrics and parallel-plate media, RE Trans. Antennas Propag. 10,82 95 (1962).

[15] C. P. Scarborough, Q. Wu, M. D. Gregory, D. H. Werner, R. K. Shaw, and E. Lier, "Broadband metamaterial soft-surface horn antennas," Proc. 2010 IEEE International Symposium on Antennas and Propagation and USNC/URSI National Radio Science Meeting, Toronto, Canada, July 11-17, 2010.

[16] E. Lier, R. K. Shaw, D. H. Werner, Q. Wu, C. P. Scarborough, and M. Gregory, "Status on meta-horn development – theory and experiments," Proceedings of the 2010 IEEE International Symposium on Antennas and Propagation and USNC/URSI National Radio Science Meeting , Toronto, Canada, July 11-17, 2010.

[17] Q. Wu, C. P. Scarborough ,, B. G. Martin, R. K. Shaw, D. H. Werner , E. Lier ,and X. Wang, “A K-u Band Dual Polarization Hybrid-Mode Horn Antenna Enabled by Printed-Circuit-Board Metasurfaces”, IEEE TRANS. ANTENNAS AND PROPAGATION, vol. 61, no. 3, pp. 1089-1098, 2013.

[18] B. A. Munk, Frequency Selective Surfaces: Theory and De-sign . Hoboken, NJ, USA: Wiley, 2000.

[19] E. Lier, D. H. Werner, C. P. Scarborough, Q. Wu, and J. A. Bossard,“An octave-bandwidth negligible-loss radiofrequency metamaterial,” Nature Mater. , vol. 10, pp. 216–222, 2011.

[20] J. Kennedy, “Encyclopedia of Machine Learning”, pp. 760-766, 2010.

[21] Q. Wu, C. P. Scarborough, D. H. Werner , E. Lier, and X. Wang, “Design Synthesis of Metasurfaces for Broadband Hybrid-Mode Horn Antennas With Enhance Radiation Pattern and Polarization Characteristics” IEEE TRANS. ANTENNAS AND PROPAGATION, vol. 60, no. 8, pp. 3594-3604, 2012.

[22] E. Lier and R. K. Shaw, “Design and simulation of metamaterial-based hybrid-mode horn antennas,” Electron. Lett. , vol. 44, pp. 1444–1445,2008.